

# Slow light using wave mixing in liquid crystal light valve

S. Residori · U. Bortolozzo · J.P. Huignard

Received: 29 January 2009 / Revised version: 5 April 2009 / Published online: 7 May 2009  
© Springer-Verlag 2009

**Abstract** By performing optical two-wave mixing in a liquid crystal light valve, we are able to slow down optical pulses to group velocities as slow as a few tenths of mm/s, corresponding to a very large group index. We present experiment and model of the slow light process occurring in liquid crystal light valves. The large group index corresponds to having a large sensitivity for phase variations, a property that can be used to increase the sensitivity of Fourier transform interferometer. We show that when a liquid crystal light valve is inserted in a Mach–Zehnder interferometer, the effect of frequency perturbations at the input of the system is amplified by a factor related to the group delay.

**PACS** 42.65.Hw · 42.50.Gy · 42.70.Df · 77.22.Gm

## 1 Introduction

The ability to slow pulses of light has recently received a large interest as a solution to the problem of pulse buffer-

ing in optical communication systems [1]. Indeed, the realization of all-optical communication networks relies on the ability to store, switch and delay optical pulses [2]. In addition, it has recently been pointed out that slowing down optical pulses can be used to enhance the spectral sensitivity of certain types of interferometers [3], which is expected to have a significant impact in applications such as precision metrology and optical sensing. Much of the early research into slow light was carried out using electromagnetically induced transparency in atomic vapors [4] or ultracold atoms [5]. More recently, a considerable deceleration of light pulses was obtained in room temperature solids, such as ruby crystals, through the quantum coherence effect [6], and in photorefractive crystals through the strong dispersion of dynamic gratings in the vicinity of Bragg resonance [7–10]. Other recent techniques employ nonlinear effects in optical fibers, such as amplification [11] or stimulated Brillouin scattering [12], or active control in photonic crystal waveguides [13].

Recently, we have shown that slow, and indeed fast, light phenomena are possible using liquid crystal light valves [14]. Liquid crystal devices offer the potential for slowing whole images, and possess unique features for practical implementations, such as a large electro-optic response, visible and near-IR transparency, small-size operating devices and widespread technological impact. In our experiments, slow and fast light phenomena were obtained by performing non degenerate two-wave mixing (TWM) in a liquid crystal light valve (LCLV) and by exploiting the dispersion properties associated with the mixing process.

In the first part of the paper we will focus on the mechanism for achieving slow light in the LCLV, by describing in detail the TWM process and by showing some representative experimental results. Then, we will present a Mach–Zehnder interferometer in which the large group index of

---

S. Residori (✉) · U. Bortolozzo  
Institut Non Linéaire de Nice, Université de Nice  
Sophia-Antipolis, CNRS, 1361 Route des Lucioles, 06560  
Valbonne, France  
e-mail: [stefania.residori@inln.cnrs.fr](mailto:stefania.residori@inln.cnrs.fr)

U. Bortolozzo  
Faculty of Mathematical, Physical and Natural Sciences,  
University of Verona, Ca' Vignal 2, Strada le Grazie 15, 37134  
Verona, Italy

J.P. Huignard  
Thales Research & Technology, RD 128, 91767 Palaiseau Cedex,  
France

the slow light process in the LCLV allows obtaining a very large sensitivity. The LCLV and its main features, are described in Sect. 2. A theoretical derivation of the gain and dispersion properties of the non degenerate TWM are provided in Sect. 3, while Sect. 4 contains a brief summary of the main experimental results. In Sect. 5 we report the enhanced response of a Mach–Zehnder interferometer (MZI) in which the LCLV acts as a slow light medium, and Sect. 6 is the conclusions.

## 2 The liquid crystal light valve working in transmission

The liquid crystal light valve is made by the association of a nematic liquid crystal layer and a photorefractive crystal [15], and has recently been demonstrated as an attractive and versatile medium for nonlinear optics [16] and beam coupling experiments [17]. The device exploits the advantages of coupling the large electro-optic effect of the photorefractive layer with the large birefringence of the nematic liquid crystals, thus leading to a high sensitivity and optical response. Moreover, at difference with other types of spatial light modulators or light valves [18], usually working in reflection and thus imposing an optical isolation between the input and readout beams, the photorefractive LCLV works in transmission, allowing an easy implementation of classical wave-interaction schemes. For instance, based on these features, optical amplification [19] and self-pumped phase-conjugation [20] in photorefractive LCLV have recently been reported.

A detailed description of the LCLV can be found in [14]. As schematically represented in Fig. 1, it essentially consists of a liquid crystal (LC) layer in between a photorefractive  $\text{Bi}_{12}\text{SiO}_{20}$  (BSO) crystal and a glass wall. Transparent electrodes (made of Indium-Tin Oxide, ITO) allow to apply an external a.c. voltage  $V_0$ , whose frequency is typically from 0.5 to 2 kHz and *rms* amplitude from 5 to 20 V. The thickness of the LC layer is fixed to  $d = 14 \mu\text{m}$  and the initial

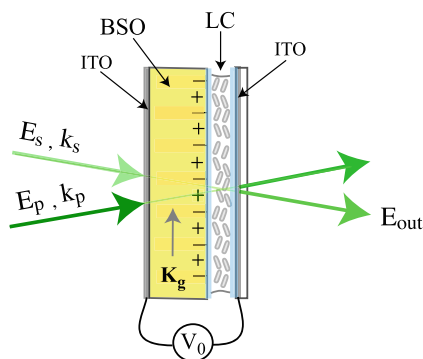


**Fig. 1** Schematic representation of the LCLV and of the two-beam coupling occurring in the liquid crystal (LC) layer. The BSO is the photoconductive wall and the ITO layers are the transparent electrodes

alignment of the LC molecules is parallel to the confining walls (planar anchoring). The BSO, which is transparent in the visible range, is here used for its large photoconductivity [21]. When the voltage is applied to the LCLV, the LC molecules tend to realign in such a way as to become parallel to the applied field. Due to the presence of the photoconductive wall, the effective voltage across the LC layer is a function of the incident light intensity [15], therefore the molecular arrangement follows the light intensity distribution on the BSO side of the LCLV.

Associated with the molecular distribution of orientation there is a refractive index change, which follows from the birefringent properties of the LC,  $n_e = 1.7$  and  $n_o = 1.5$  being the extraordinary and, respectively, the ordinary refractive index. Hence, at the exit of the LCLV the light beam acquires a phase shift that is a function of the light intensity itself and of the applied voltage  $V_0$ . For low intensities, less than  $5 \text{ mW}/\text{cm}^2$ , the phase retardation scales linearly with the intensity and the device behaves as a Kerr-like nonlinear medium.

### 2.1 Optical response of the LCLV

Because of the LC birefringence, the molecular reorientation under the action of an impinging beam implies a refractive index change  $\Delta n$ , which depends on the light intensity itself. A typical response of the LCLV is displayed in Fig. 2. A probe beam is sent to the LCLV together with a pump beam. The phase change experienced by the probe beam,  $\varphi = 2\pi \Delta n d / \lambda$ , is measured at the output of the valve by recording the displacements of the fringe patterns in an interferometric setup, and is plotted in Fig. 2 as a function of the pump intensity  $I_p$ . A large linear part of the response is obtained for small pump intensity. The phase change decreases from  $13\pi$  to 0, correspondingly the refractive index change decreases from the maximum value of the LC birefringence  $\Delta n = n_e - n_o = 0.2$  to zero, which occurs when all the liquid crystal molecules are aligned along the direction of the applied field and give the saturation of the response.

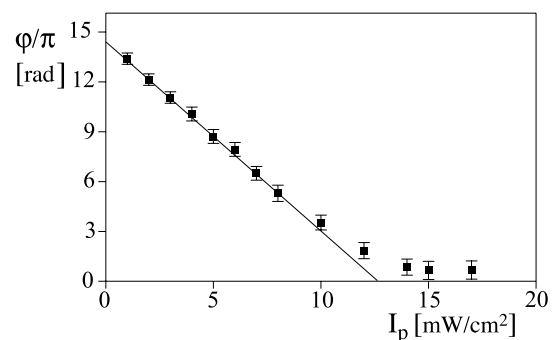


**Fig. 2** Phase retardation induced by the LCLV on the probe beam, as a function of the pump intensity  $I_p$

Therefore, in the linear part of the response the LCLV behaves as a Kerr-like nonlinear medium, providing a refractive index change  $\Delta n \propto I_p$ . For an incident illumination of a few mW/cm<sup>2</sup>, the typical response time is of the order of 100 ms, which is the time needed for the molecular reorientation to establish over the LC layer.

### 3 Dispersive properties of the two-wave mixing in the LCLV

The basic scheme of the two-wave mixing in the LCLV is represented in Fig. 1. A high-intensity pump beam,  $E_p$ , together with a weaker signal,  $E_s$ , both enlarged and collimated with a waist of 18 mm and propagating with respective wave vectors  $\mathbf{k}_p$  and  $\mathbf{k}_s$ , are sent to interfere onto the LCLV, where they produce an intensity fringe pattern. The ratio between the pump and signal intensities, usually much larger than one, is defined as  $\beta \equiv I_p/I_s$ , with  $I_p = |E_p|^2$  and  $I_s = |E_s|^2$ , and is a parameter of the experiment. The fringe spacing is usually varied from 100 to 300  $\mu\text{m}$ .

The total electric field  $E_{\text{in}}$  at the input of the LCLV can be written as

$$E_{\text{in}}(\mathbf{r}, t) = E_s e^{i[\mathbf{k}_s \cdot \mathbf{r} - \omega_s t]} + E_p e^{i[\mathbf{k}_p \cdot \mathbf{r} - \omega_p t]} + \text{c.c.}, \tag{1}$$

where  $\omega_s$  and  $\omega_p$  are the frequencies of the signal and the pump beam, respectively, and

$$\delta = \omega_p - \omega_s \tag{2}$$

is the frequency detuning. The two beams give rise to an intensity fringe pattern

$$|E_{\text{in}}(\mathbf{r}, t)|^2 = |E_s|^2 + |E_p|^2 + 2E_p E_s \cos((\mathbf{k}_p - \mathbf{k}_s) \cdot \mathbf{r} - \delta t), \tag{3}$$

which, through the photoconductive effect, induces a molecular reorientation pattern in the liquid crystal layer and, hence, to a refractive index grating with the same wave vector  $\mathbf{K}_g = \mathbf{k}_p - \mathbf{k}_s$  and spatial period  $\Lambda \equiv 2\pi/K_g$ .

The amplitude  $n(\mathbf{r}, t)$  of the refractive index grating is governed by a Debye relaxation equation [22]

$$\tau_{\text{LC}} \frac{\partial n}{\partial t} = -(1 - l_d^2 \nabla^2)n + n_c + n_2 |E_{\text{in}}|^2 \tag{4}$$

that follows from the relaxation dynamics of the LC molecules, where  $\tau_{\text{LC}}$  is the LC relaxation time,  $l_d$  is the transverse diffusion length due to elastic coupling in the LC and charge diffusion in the photoconductive layer,  $n_c$  is the constant value of the refractive index that is given by the average LC orientation under the application of the  $V_0$  voltage, and  $n_2$  is the equivalent Kerr-like coefficient of the LCLV [19].

By coupling the above equation, (4), with the wave equation for the propagation of light in a medium with refractive index  $n$ ,

$$\nabla^2 E - \left(\frac{n}{c}\right)^2 \frac{\partial^2 E}{\partial t^2} = 0, \tag{5}$$

with boundary conditions given by (1),  $E = E_{\text{in}}$  at  $z = 0$ , we obtain the output signal beam.

Note that the liquid crystal layer is thin with respect to the fringe spacing, so that the beam coupling occurs in the Raman–Nath regime of diffraction. This is different from previous experiments in bulk photorefractive crystals, where the TWM occurs in the Bragg regime [7–10]. In the Raman–Nath regime, it is well known that the output field can be written as a series of Bessel function, corresponding to the multiple scattered orders [23]. The expression for all the  $m$  output orders at the exit of the LCLV is reported in [24, 25]. In the direction of the signal, which is of the zero output order, the output field is given by

$$E_{\text{out}} = [E_s J_0(\rho) + i E_p J_1(\rho) e^{-i\Psi}] \times e^{i[k(n_c + kn_2 I_{\text{in}})z]} e^{i(\mathbf{k}_s \cdot \mathbf{r} - \omega_s t)} + \text{c.c.}, \tag{6}$$

where

$$\rho = \frac{2kn_2 E_p E_s}{\sqrt{(1 + l_d^2 K_g^2)^2 + (\delta \tau_{\text{LC}})^2}} d, \tag{7}$$

$$\tan \Psi = \frac{\delta \tau_{\text{LC}}}{1 + l_d^2 K_g^2}, \tag{8}$$

and  $J_m$  is the Bessel function of the first kind and of order  $m$ . It can be easily recognized that  $J_0$  accounts for the scattering of the signal onto itself and  $J_1$  for the scattering of the pump in the direction of the signal.

The output signal beam can thus be written as

$$E_{\text{out}} = \sqrt{G I_s} e^{i\Phi} e^{i(\mathbf{k}_s \cdot \mathbf{r} - \omega_s t)} + \text{c.c.} \tag{9}$$

where  $G$  is the two-wave mixing gain and  $\Phi$  the nonlinear phase shift. A simplified expression can be written when  $\rho \ll 1$ . In this case, the TWM gain  $G = |E_{\text{out}}|^2/I_s$  is given by

$$G = 1 + 2g \sin(\Psi)d + g^2 d^2 \tag{10}$$

where

$$g = \frac{kn_2 I_p}{\sqrt{(1 + l_d^2 K_g^2)^2 + (\delta \tau_{\text{LC}})^2}}, \tag{11}$$

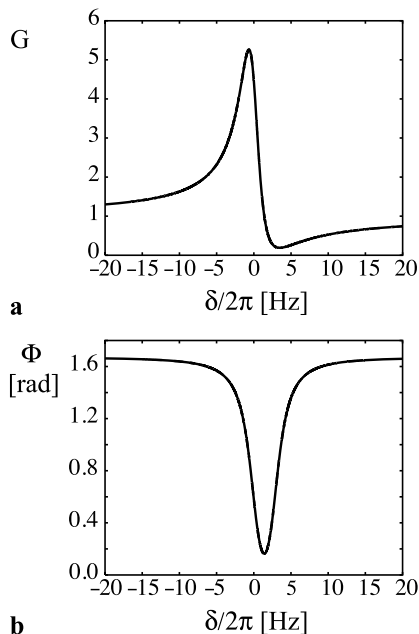


**Fig. 3** **a** Gain  $G$  and **b** phase shift  $\Phi$  for the output beam, each as a function of the frequency detuning  $\delta$  between the pump and signal,  $\beta = 80$

and the phase shift is given by

$$\Phi = \tan^{-1} \left( \frac{kn_2 I_p \cos(\Psi)d}{\sqrt{(1 + l_d^2 K_g^2)^2 + (\delta\tau_{LC})^2 + kn_2 I_p \sin(\Psi)d}} \right) + k[n_c + n_2 I_{in}]d. \tag{12}$$

$G$  and  $\Phi$  are plotted in Fig. 3 a and b, respectively, each as a function of the frequency detuning  $\delta$ . The values of the parameters, chosen by following the typical experimental conditions, are  $\tau_{LC} = 120$  ms,  $l_d = 14$   $\mu\text{m}$ ,  $\Lambda = 250$   $\mu\text{m}$ ,  $n_2 = -6$   $\text{cm}^2/\text{W}$ ,  $I_p = 2$   $\text{mW}/\text{cm}^2$  and  $\beta = 80$ . Note that for  $\delta = 0$  and in the limit  $l_d^2 K_g^2 \ll 1$ , a condition that is often satisfied in the experiments,  $G$  reduces to the simple expression

$$G = 1 + \left( \frac{2\pi n_2 I_p}{\lambda} \right)^2 d^2, \tag{13}$$

as already derived in [26].

Experimentally, we can measure  $G$  as the ratio of the output to the input signal intensity and, by using the above expression (10), we can derive the nonlinear coefficient  $n_2$ . As an example, we report in Fig. 4 the  $n_2$  measured as a function of the voltage  $V_0$  applied to the LCLV and for different pump intensities. In this set of measurements the frequency of the applied voltage was 1 kHz. The large value of  $n_2$  reflects the large and slow nonlinear response of the LCLV.

The strength of the nonlinearity can be tuned by varying the voltage  $V_0$  applied to the LCLV. From the phase response, previously calculated, the group delay of the out-

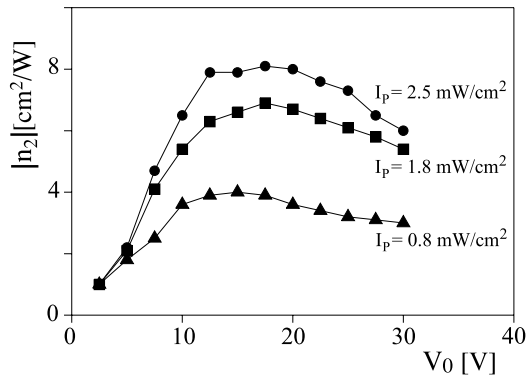


**Fig. 4** LCLV nonlinear coefficient  $n_2$  measured as a function of the voltage  $V_0$ ,  $f = 1$  kHz, and for different pump intensities

put signal beam in the case of degenerate two-wave mixing ( $\delta = 0$ ) is

$$\tau_g = \frac{\partial \Phi}{\partial \omega_s} = \tau_{LC} \frac{(\beta k_0 d n_2 I_p)^2}{1 + (\beta k_0 d n_2 I_p)^2}, \tag{14}$$

where we have considered  $l_d \ll 2\pi/K_g$  and that the LCLV is supposed to work in the linear part of its optical response; that is, the pump intensity  $I_p$  has to be kept less than 10  $\text{mW}/\text{cm}^2$  (see Fig. 2). Correspondingly, for an input signal of a few  $\mu\text{W}/\text{cm}^2$ , a maximum value of  $\beta \sim 10^4$  can be used. However, for the high  $n_2$  coefficient of the LCLV and typical values of  $I_p$ , the phase shift  $k_0 d n_2 I_p$  is of the order one and the maximum value of  $\tau_g = \tau_{LC}$  is already reached for values of  $\beta$  less than 10. Moreover, the group delay depends on the two-wave mixing gain; thus, by changing the voltage  $V_0$  applied to the LCLV, it can be tuned from 0 to the maximum value  $\tau_{LC}$ .

#### 4 Slow light in the LCLV: experimental results

The experimental setup is a two-wave mixing, as represented in Fig. 1, where the pump beam is sent onto the LCLV together with a light pulse as a signal. The pump and signal originating from the same laser, a cw doubled diode-pumped solid state at  $\lambda = 532$  nm, are polarized linearly and parallel to the LC initial orientation, and are enlarged and collimated with a waist of 18 mm. The intensity of the pump is  $I_p = 1.8$   $\text{mW}/\text{cm}^2$ , whereas the signal beam is time-modulated, by means of a spatial-light modulator, to obtain a Gaussian wave packet with a width larger than the LC response time and a peak intensity  $I_s$ . The beam intensity ratio  $\beta \equiv I_p/I_s$  is fixed to 30. The center frequency of the signal can be changed by a few Hz with a piezoelectrically driven mirror.

As we have shown in [14], different group delays can be obtained on the different output orders originating from the beam coupling in the Raman–Nath regime of diffraction.

Here, we focus on the  $m = 0$  order, which is the output beam propagating in same direction as the input signal. In Fig. 5 we show two representative experimental data, displaying the slow light behavior of the output beam for two different values of the voltage  $V_0$ . The input pulse width is 140 ms and the frequency detuning  $\delta = 0$  Hz. The fringe spacing and, correspondingly, the period of the refractive index grating is 110  $\mu\text{m}$ . For better visualization of the temporal shift, all the intensities are normalized to their peak value. In reality, the slow light pulses are amplified due to the TWM gain, which is measured as the ratio of the output to the input peak intensity and is about 4. By fitting each pulse with a Gaussian, we evaluate the group delay as  $\tau_g = 64$  ms for (a)  $V_0 = 20$  V and  $\tau_g = 90$  ms for (b)  $V_0 = 24$  V, which is close to the predicted maximum group delay  $\tau_{LC}$ . Correspondingly, the group velocity  $v_g = d/\tau_g$ , is 0.22 mm/s for (a)  $V_0 = 20$  V and (b) 0.16 mm/s for  $V_0 = 24$  V. Such small values of the group velocity imply a very large group index that can be used for enhancing the sensitivity of interferometric systems, as we will show in the next section. To avoid distortions/broadening of the output pulse, the width of the input pulse has been kept less than the LC response time  $\tau_{LC}$ . Therefore, the maximum fractional delay achievable is 1, a limitation that is a common problem in slow light systems [2].

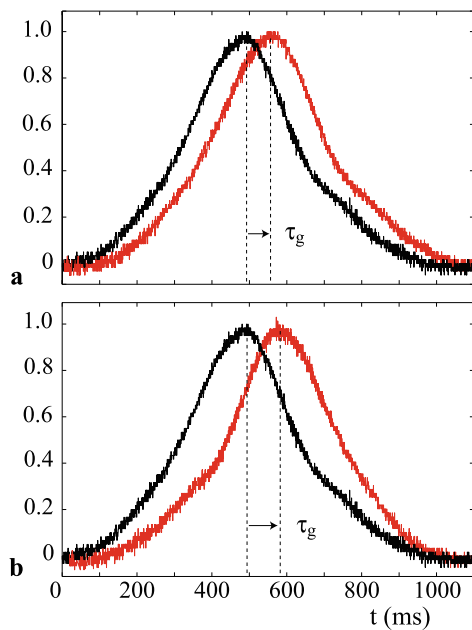


**Fig. 5** Experimental time dependencies (red lines) of the output pulse for **a**  $V_0 = 20$  V and **b**  $V_0 = 24$  V,  $f = 1$  kHz. The input pulse is the black line. The group delay  $\tau_g$  is marked by the arrow

### 5 Enhanced response of a Mach–Zehnder interferometer with an LCLV as a slow light medium

Compact interferometers with high spectral sensitivity or resolution are becoming more and more desired in various applications, such as metrology, optical sensing, quantum information processing, and biomedical engineering.<sup>1</sup> Recently, it has been shown that slow light can be used to enhance the spectral sensitivity of certain types of interferometers [3, 27]. In the ideal case of lossless slow light medium and of uniform group index over the bandwidth of interest, the spectral sensitivity or resolution is enhanced by a factor equal to the group index  $n_g$  of the slow light medium. In the case of the LCLV,  $n_g$  can become as large as of the order of  $10^{11}$ . At the same time, the two-wave mixing process is preventing losses and provides a gain that is tunable with the applied voltage, so that the slow light interferometer can be adjusted to work in optimal conditions.

We have realized a Mach–Zehnder interferometer in which an LCLV is inserted in one of the arms. The experimental setup is sketched in Fig. 6. The output signal is present even when the LCLV is not operating, and we can make a direct comparison between the sensitivity with and without the slow light effect. The transmission of the interferometer is given by

$$T = \frac{1}{2}[1 + \cos \Delta\Phi] \tag{15}$$

where the total phase difference  $\Delta\Phi$  between the two arms is given by the optical path length difference  $\Delta L$  and by the slow light nonlinear phase retardation  $\Phi$ , which is a function of the frequency detuning, as we have seen in Sect. 3.

Now, if we introduce on the input signal a frequency perturbation  $\Omega$ , which is small with respect to the bandwidth of the two-wave mixing,  $B = 1/2\tau_{LC}$ , we can write

$$\Phi(\Omega) \simeq \Phi(0) + \left[ \frac{\partial\Phi}{\partial\Omega} \right]_{\Omega=0} \Omega, \tag{16}$$

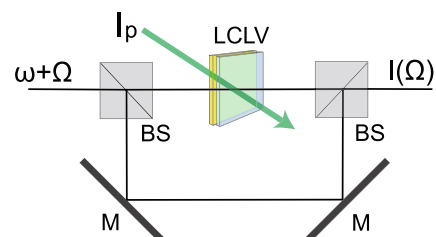


**Fig. 6** Schematic diagram of a Mach–Zehnder interferometer employing an LCLV as a slow light medium

<sup>1</sup>See, e.g., [3] and references therein.

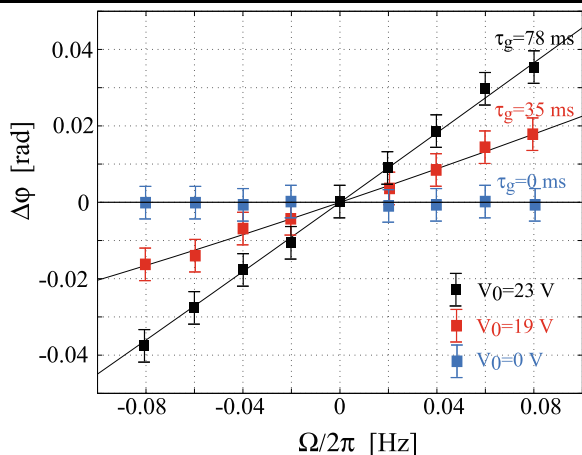


**Fig. 7** Phase detected by the MZI as a function of the perturbation frequency  $\Omega$ , for different voltages  $V_0$  applied to the LCLV and correspondingly increasing group delays

and the total phase difference  $\Delta\Phi(\Omega)$  can be rewritten as

$$\Delta\Phi(\Omega) = \frac{\Omega}{c} \Delta L + \tau_g \Omega. \quad (17)$$

When the LCLV is operating, the slow light contribution is much higher than the first term and the above expression reduces to

$$\Delta\Phi = \tau_g \Omega, \quad (18)$$

so that the frequency sensitivity of the interferometer is directly related to the group delay of the slow light medium. The spectral sensitivity of the interferometer can be quantified as the rate at which  $\Delta\Phi$  changes with the frequency  $\Omega$ , so that

$$\frac{d\Delta\Phi}{d\Omega} = \tau_g = \frac{dn_g}{c}, \quad (19)$$

with  $n_g$  the group index.

In Fig. 7 we report the phase detected at the output of the interferometer when a small perturbation of frequency  $\Omega$  is added on the input laser beam. The perturbation is created through a piezoelectrically driven mirror. We can see that when the LCLV is switched on ( $V_0 \neq 0$ ), the sensitivity increases with increasing the group delay, in agreement with the theoretical prediction. Owing to the large group index provided by the LCLV, the MZI shows a large sensitivity. Moreover, in the LCLV the slow light effect does not critically depend on the incident wavelength, which is an advantage with respect to other slow light media that are very dispersive but also resonant in wavelength. In other words, the same setup can be used to detect very small frequency perturbations around different carrier wavelengths, the transparent photoconductor of the LCLV giving an optimized response in between 400 to 550 nm and, thus, the TWM working for different wavelengths in this spectral range.

## 6 Conclusions

In conclusion, transmissive LCLVs are attractive devices showing large and tunable nonlinear response and excellent photosensitivity coming from the association of the photoconductive layer with the large birefringence of the liquid crystals. Here, we have shown that by performing two-wave mixing experiments in LCLVs, and by using the dispersive properties associated with the two-beam coupling process, we can obtain slow light phenomena with very large group delay. The corresponding group index, which is as large as  $10^{11}$ , has been exploited to enhance the sensitivity of a Mach–Zehnder interferometer.

**Acknowledgements** This work has been partially supported by the ANR-07-BLAN-0246-03, *turbonde*.

## References

1. F. Xia, L. Sekaric, Y. Vlasov, *Nat. Photonics* **1**, 65 (2007)
2. R.W. Boyd, D.J. Gauthier, in *Progress in Optics*, vol. 43, ed. by E. Wolf (Elsevier Science, Amsterdam, 2002), pp. 497–530
3. Z. Shi, R.W. Boyd, D.J. Gauthier, C.C. Dudley, *Opt. Lett.* **32**, 915 (2007)
4. A. Kasapi, M. Jain, G.Y. Yin, S.E. Harris, *Phys. Rev. Lett.* **74**, 2447 (1995)
5. L.V. Hau, S.E. Harris, Z. Dutton, C.H. Behroozi, *Nature* **397**, 594 (1999)
6. M.S. Bigelow, N.N. Lepeshkin, R.W. Boyd, *Phys. Rev. Lett.* **90**, 113903 (2003)
7. E. Podivilov, B. Sturman, A. Shumelyuk, S. Odoulov, *Phys. Rev. Lett.* **91**, 083902 (2003)
8. A. Shumelyuk, K. Shcherbin, S. Odoulov, B. Sturman, E. Podivilov, K. Buse, *Phys. Rev. Lett.* **93**, 243604 (2004)
9. G. Zhang, R. Dong, F. Bo, J. Xu, *Appl. Opt.* **43**, 1167 (2004)
10. F. Bo, G. Zhang, J. Xu, *Opt. Express* **13**, 8198 (2005)
11. G.M. Gehring, A. Schweinsberg, C. Barsi, N. Kostinski, R.W. Boyd, *Science* **312**, 895 (2006)
12. M. González-Herráez, K.-Y. Song, L. Thévenaz, *Appl. Phys. Lett.* **87**, 081113 (2005)
13. Y.A. Vlasov, M. O’Boyle, H.F. Hamann, S.J. McNab, *Nature* **428**, 65 (2005)
14. S. Residori, U. Bortolozzo, J.P. Huignard, *Phys. Rev. Lett.* **100**, 203603 (2008)
15. P. Aubourg, J.P. Huignard, M. Hareng, R.A. Mullen, *Appl. Opt.* **21**, 3706 (1982)
16. U. Bortolozzo, S. Residori, J.P. Huignard, *J. Nonlinear Opt. Phys. Mater.* **16**(2), 231 (2007)
17. U. Bortolozzo, S. Residori, J.P. Huignard, *J. Phys. D: Appl. Phys.* **41**, 224007 (2008)
18. U. Efron, G. Liverscu, in *Spatial Light Modulator Technology: materials, devices and applications*, ed. by U. Efron (Marcel Dekker, New York, 1995)
19. U. Bortolozzo, S. Residori, J.P. Huignard, *Opt. Lett.* **31**, 2166 (2006)
20. U. Bortolozzo, S. Residori, J.P. Huignard, *Opt. Lett.* **32**, 829 (2007)

21. P. Gunter, J.P. Huignard, *Photorefractive Materials and Their Applications 1* (Springer, New York, 2006)
22. P.G. De Gennes, J. Prost, *The Physics of Liquid Crystals*, 2nd edn. (Oxford Science Publications/Clarendon, London, 1993)
23. A. Yariv, *Optical Waves in Crystals* (Wiley, New Jersey, 2003)
24. U. Bortolozzo, A. Montina, F.T. Arcelli, J.P. Huignard, S. Residori, Phys. Rev. Lett. **99**, 023901 (2007)
25. A. Montina, U. Bortolozzo, S. Residori, J.P. Huignard, Phys. Rev. A **76**, 033826 (2007)
26. A. Brignon, I. Bongrand, B. Loiseaux, J.P. Huignard, Opt. Lett. **22**, 1855 (1997)
27. Z. Shi, R.W. Boyd, in *Proceedings of the 2008 OSA: COTA/ICDI/IPNRA/SL, SWA3*, 2008